Proceedings of the 30th International Cosmic Ray Conference
Rogelio Caballero, Juan Carlos D'Olivo, Gustavo Medina-Tanco,
Lukas Nellen, Federico A. Sánchez, José F. Valdés-Galicia (eds.)
Universidad Nacional Autónoma de México,
Mexico City, Mexico, 2008
Vol. 2 (OG part 1), pages 3–6

30TH INTERNATIONAL COSMIC RAY CONFERENCE

ICRC'07
Mérida, México

Relative abundances of cosmic ray nuclei B-C-N-O in the energy region from 10 GeV/n to 300 GeV/n. Results from ATIC-2 (the science flight of ATIC).

A. D. PANOV[1], N. V. SOKOLSKAYA[1], J. H. ADAMS, JR.[2], H. S. AHN[3], G. L. BASHINDZHAGYAN[1], K. E. BATKOV[1], J. CHANG[4,5], M. CHRISTL[2], A. R. FAZELY[6], O. GANEL[3], R. M. GUNASINGHA[6], T. G. GUZIK[7], J. ISBERT[7], K. C. KIM[3], E. N. KOUZNETSOV[1], M. I. PANASYUK[1], W. K. H. SCHMIDT[5], E. S. SEO[3], J. WATTS[2], J. P. WEFEL[7], J. WU[3], V. I. ZATSEPIN[1].
[1]*Skobeltsyn Institute of Nuclear Physics, Moscow State University, Moscow, Russia*
[2]*Marshall Space Flight Center, Huntsville, AL, USA*
[3]*University of Maryland, Institute for Physical Science & Technology, College Park, MD, USA*
[4]*Purple Mountain Observatory, Chinese Academy of Sciences, China*
[5]*Max-Planck Institut for Solar System Research, Katlenburg-Lindau, Germany*
[6]*Southern University, Department of Physics, Baton Rouge, LA, USA* [7]*Louisiana State University, Department of Physics and Astronomy, Baton Rouge, LA, USA*
panov@dec1.sinp.msu.ru

Abstract: The ATIC balloon-borne experiment measures the energy spectra of elements from H to Fe in primary cosmic rays from about 100 GeV to 100 TeV. ATIC is comprised of a fully active bismuth germanate calorimeter, a carbon target with embedded scintillator hodoscopes, and a silicon matrix that is used as the main charge detector. The silicon matrix produces good charge resolution for protons and helium but only partial resolution for heavier nuclei. In the present paper, the charge resolution of ATIC was improved and backgrounds were reduced in the region from Be to Si by using the upper layer of the scintillator hodoscope as an additional charge detector. The flux ratios of nuclei B/C, C/O, N/O in the energy region from about 10 GeV/nucleon to 300 GeV/nucleon obtained from this high-resolution, high-quality charge spectra are presented, and compared with existing theoretical predictions.

Introduction

The ATIC spectrometer, its calibration and the algorithm of trajectory reconstruction have been described [1, 2, 3]. Charge resolution provided by the silicon matrix is sufficient to obtain spectra of primary protons and helium [4, 5] and preliminary spectra of some abundant heavy nuclei [6, 5].

Very important to understand the mechanism of propagation of cosmic rays in the Galaxy is the boron (which is a secondary nuclide) to carbon ratio in cosmic rays. The problem of B/C ratio has been experimentally investigated in the energy range 0.5–50 GeV/n (see [7] and references herein). The energy range of the ATIC experiment allow data for higher energies (up to 200–300 GeV/n) to be obtained. But there are obstacles: 1) low charge resolution of the silicon matrix in the range of charges 5-8 and 2) high background in the silicon matrix charge spectrum in the range of boron and carbon (see fig. 1). In this paper we use the upper layer of the scintillator hodoscope to improve the charge resolution and to reduce backgrounds in B-C region to measure B/C in the ATIC experiment.

Improved charge spectrum

The upper scintillator layer of the hodoscope is comprised by 42 parallel scintillator strips $1 \times 2 \times 88.2\ \mathrm{cm}^3$. Using these scintillators as a supplementary charge detector, involves a multi-step procedure of calibration and normalization of the signals which will be described in detail elsewhere. In brief, the method is the following. The first step is to use the usual method to measure the charge of

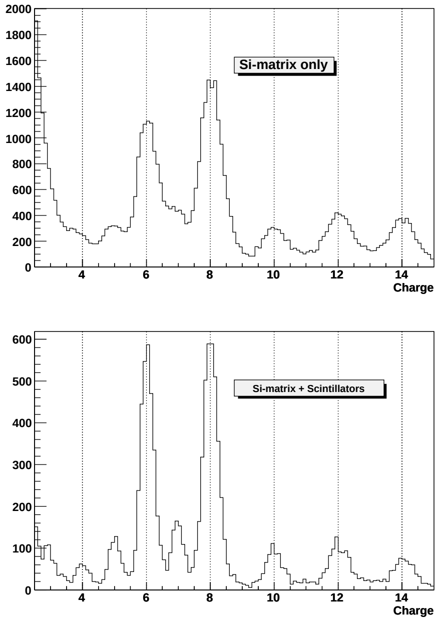

Figure 1: The charge spectra obtained with the silicon matrix only and with the silicon matrix plus the upper layer of hodoscope for the range of energy deposit in BGO calorimeter 50–100 GeV (primary energy per particle approximately 150–300 GeV)

primary particles – trajectory reconstruction from signals in BGO-calorimeter project - to the silicon matrix. The charge detected in the silicon matrix (Q_{Si}) is the maximal signal in the area of confusion for the trajectory [1, 2, 3]. In the second step, we find the charge detected in each scintillator strip and select the strip with the charge nearest to the charge detected by the silicon matrix (Q_{Sci}). This charge is accepted if the distance from the strip to the reconstructed trajectory is less than 5cm and is rejected otherwise. In the third step, an event is rejected if $|Q_{\text{Sci}} - Q_{\text{Si}}| > 0.25$. The final result for the charge is $Q = (Q_{\text{Sci}} + Q_{\text{Si}})/2$. This procedure reduces the backgrounds in the charge spectrum and improves its resolution, but reduces the initial statistics by a factor of about 4. There are other strategies to process charge data from the scintillator hodoscope, but for this paper we select the strategy of "higher resolution - lower backgrounds - lower statistics". The charge spectra obtained with the silicon matrix only and with the silicon matrix plus the upper layer of hodoscope are compared in fig. 1.

Measurement of the relative fluxes

We calculate the ratio of fluxes of different nuclei in cosmic rays to the flux of carbon against energy of particles per nucleon. It is a multi-step procedure which is designed to obtain the most exact information for fluxes of nuclei with charges $4 \leq q \leq 14$.

1. For five ranges of the energy deposit E_d in the BGO calorimeter (50–100, 100–200, 200–398, 398–794, 794–1585 GeV) we obtain the charge spectra (similar to fig. 1, lower graph), and decompose each by Gaussian fits (the value χ^2 per degree of freedom is close to 1 in all cases). The positions of peaks are determined and charge cuts are developed for each particular primary particle such that the margins of cuts are at the half of path between adjacent peaks. The number of counts $I^0_{s,q}$ in each charge bin q for E_d range number s is the raw data to obtain the fluxes of primary particles ($s = 0$ corresponds to the energy region of E_d 50–100 GeV, etc).

2. Protons and helium interacting in the material (aluminum honeycomb and other) of ATIC above the silicon matrix can sometimes simulate heavier nuclei. This effect is energy dependent (grows with energy). Corresponding backgrounds $B^{\text{p,He}}_{s,q}$ for each value $I^0_{s,q}$ are calculated by simulation of propagation of protons and helium through the ATIC instrument by the FLUKA code [8], with simulation of the conditions of charge selection (see previous section). The apparatus charge line widths are accounted for as well. This procedure produces the corrected values of intensities $I^1_{s,q} = I^0_{s,q} - B^{\text{p,He}}_{s,q}$. The value of $B^{\text{p,He}}_{s,q}$ for boron $(q = 5)$ varies from 9% to 36% of $I^0_{s,q}$.

3. Particles with charges $q \geq 15$ fragmenting in the material above the silicon matrix can also produce nuclei of $4 \leq q \leq 14$. The corresponding backgrounds were subtracted but the effect is small (about 0.1% for boron) and we do not describe the method of subtraction here.

4. Each nuclei of $4 \leq q \leq 14$ due to interactions in ATIC, and due to the apparatus broadening of the peaks, produces a "charge response" of the

device which may be described for each particular nucleus q at the entrance to the instrument by a set of the coefficients $K_4^q, K_5^q, \ldots, K_{14}^q$, where K_4^q is the probability to find nucleus q in the charge bin 4, etc. Of course the coefficient K_q^q dominates strongly in the set $K_4^q, \ldots, K_{14}^q$. In other words the matrix $||K_{q'}^q||$ is diagonally-dominated. Let F_q be the intensity of the nucleus q at the entrance to ATIC. Then, for each energy region s, the experimental charge spectrum I_q^1 after subtraction of p-He backgrounds (described above; here, we do not write the index s for simplicity) may be written as

$$\begin{array}{l} I_4^1 = K_4^4 F_4 + K_4^5 F_5 + \ldots + K_4^{14} F_{14} \\ \ldots\ldots\ldots\ldots\ldots\ldots\ldots\ldots\ldots\ldots\ldots \\ I_{14}^1 = K_{14}^4 F_4 + K_{14}^5 F_5 + \ldots + K_{14}^{14} F_{14} \end{array} \qquad (1)$$

Eq. (1) is a square linear system relative to unknown values $F_4, F_5, \ldots, F_{14}$ with diagonally-dominated matrix elements, and it can be easily solved by usual methods. The coefficients of the system $K_{q'}^q$ are calculated by simulation of propagation of different nuclei through ATIC with FLUKA and the values I_q^1 are already known after steps 2 and 3. The ratio of B/C (calculated as the ratio of the contents of the related charge bins) reduced by 14%–42% for different energies.

5. The next step is a transition from the spectra of fluxes as a functions of E_d (the result of step 4) to the spectra in primary energy per nucleon. For each nucleus this procedure includes firstly a calculation of expected primary energy for each edge of the region of E_d (see step 1). To solve this problem FLUKA simulation of energy deposition was used with supposition of the primary differential momentum spectra to be a power law with index $\gamma = -2.6$ (there is only a weak dependence of exact value of γ). After normalization of the primary energy to the atomic weight and to the width of the related energy region, the fluxes of different nuclei have different energy per nucleon binning. To obtain the ratio of fluxes at the same energy we calculate the energy points obtained as a geometrical mean for the corresponding points for boron and carbon and calculate all fluxes for these energy points by interpolation of the spectrum of each nucleus. This procedure increases B/C ratio from step 4 by 13%–23% (different for different energies).

6. The mean altitude of the flight of ATIC-2 was 36.5 km which corresponds to 4.87 g/cm^2 of residual atmosphere. To obtain the primary fluxes above the atmosphere, the interaction of nuclei in the atmosphere should be accounted for. The interaction may be described as fragmentation of nuclei without changing the energy per nucleon. Then the interaction for each primary energy and for each primary nucleus q may be described by a set of coefficients $L_{q'}^q, q' \le q$ which show the probability to find the nucleus q' at the entrance of the instrument. The coefficients $L_{q'}^q$ were calculated by simulation of propagation of nuclei in the atmosphere by FLUKA. Let ψ_q be the flux of nucleus q in energy per nucleon at the entrance of ATIC (these values are known after step 5; we omit the index of the energy for simplicity) and φ_q be the same values above the atmosphere for some definite energy per nucleon. Then one can write

$$\begin{array}{l} \psi_4 = L_4^4 \varphi_4 + \ldots + L_4^{14} \varphi_{14} + \varepsilon_4 \\ \ldots\ldots\ldots\ldots\ldots\ldots\ldots\ldots \\ \psi_{14} = L_{14}^{14} \varphi_{14} + \varepsilon_{14}, \end{array} \qquad (2)$$

where $\varepsilon_4, \ldots, \varepsilon_{14}$ are small corrections related to the fragmentation of nuclei heavier than silicon $(q = 14)$. If ε_q are known then the system (2) is a square linear system relative to $\varphi_4, \ldots, \varphi_{14}$ with the triangle and diagonally-dominated matrix $L_{q'}^q$ and it can be solved directly starting from the final equation. The atmospheric correction reduces B/C ratio by 13%–33% for different primary energies.

The experimental errors were calculated as a combination of the Poisson dispersion of the experimental statistics and the statistical errors of the simulations. If the desired quantities were obtained as a solution of a linear system (as in steps 4 and 6) then corresponding complete covariation matrix were calculated by the Monte Carlo method. All reported errors are standard deviations.

Results and discussion

The results for B/C, N/O, C/O ratio are presented in table 1. The data for B/C, N/O and C/O ratio along with the data of HEAO-3-C2 experiment [7] with theoretical predictions are shown in fig. 2. One can see that the data of present work for B/C and N/O is somewhat above the data of [7] but is extended to higher energies. The theoretical curves in fig. 2 are calculations in leaky box approximation. The dashed line is based on the HEAO-3-C2

Table 1: B/C, N/O, C/O ratios as a function of primary energy (GeV/n). The numbers in parenthesis give the uncertainty in the last significant digits quoted.

E	B/C	N/O	C/O
19.9	0.180(11)	0.219(10)	1.020(26)
38.3	0.169(15)	0.199(13)	1.087(43)
74.3	0.119(29)	0.184(24)	0.933(60)
149	0.156(53)	0.172(39)	0.934(105)
307	0.064(63)	0.144(68)	1.022(227)

fit for the Galaxy escape length [7] $\lambda_{\rm esc}$=$34.1\beta R^{-0.60}$ g cm^{-2} (R is the rigidity) and the solid line is for the escape length obtained in the model of Kolmogorov type of magnetic turbulence and reacceleration during propagation [9]: $\lambda_{\rm esc} = 4.2(R/R_0)^{-1/3}\left[1+(R/R_0)^{-2/3}\right]$ g cm^{-2}, where $R_0 = 5.5$ GV. Whereas the experimental data support general trend of decreasing B/C and N/O ratio with energy, it is impossible to distinguish between different models of propagation of particles due to the experimental uncertainties.

It should be noted that our experimental data are model dependent due to extensive simulation of the backgrounds by the FLUKA code, but this could be improved by usage of additional simulation codes. One can expect that the experimental separation between different models of propagation would be possible with additional experiments.

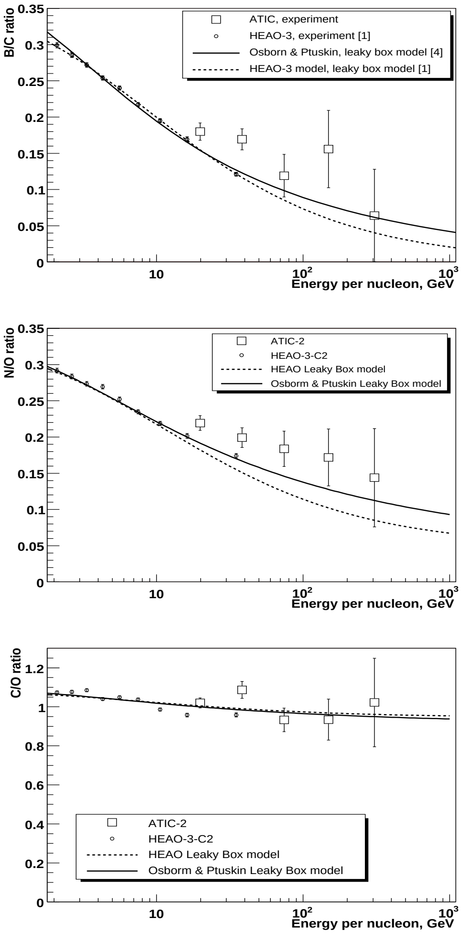

Figure 2: B/C, N/O and C/O (top-down) ratio from this work, from HEAO-3-C2 experiment and from leaky box models.

Acknowledgments

This work was supported by RFBR Grant 05-02-16222 in Russia and NASA Grants Nos. NNG04WC12G, NNG04WC10G, NNG04WC06G in the USA.

References

[1] T. G. Guzik et al. (ATIC Collaboration). *Adv. Sp. Res.*, 33(10):1763, 2004.

[2] V. I. Zatsepin et al. (ATIC Collaboration). *Nucl. Instr. Meth. A*, 524:195, 2004.

[3] N. V. Sokolskaya et al. *Phys. Atom. Nucl.*, 68:1176, 2005.

[4] J. P. Wefel et al. (ATIC Collaboration). In *29th ICRC*, V.3, P.105, 2005.

[5] A. D. Panov et al. (ATIC Collaboration). *Bull. Russ. Acad. Sc.: Physics*, 71:494, 2007.

[6] A. D. Panov et al. (ATIC Collaboration). *Adv. Sp. Res.*, 37:1944, 2006.

[7] J. J. Engelmann et al. (HEAO Collaboration). *Astron. Astrophys.*, 233:96, 1990.

[8] A. Fassò et al. arXiv:hep-ph/0306267, 2003.

[9] J. L. Osborn and V. S. Ptuskin. Sov. Astron. Lett. 14(2):132, 1988.